Gait cycle modeling in cerebral palsy condition

Sabrina Otmani, Guilhem Michon, Bruno Watier

Gait cycle modeling in cerebral palsy condition

Sabrina OTMANI[1,2], Guilhem MICHON[1], Bruno WATIER[2]

***Abstract*— Autonomous gait is a fundamental element for access to independent life and avoiding the de-socialization of people with motor disabilities. In this context, this research is part of the EXOKID project which aims at designing a personalized exoskeleton for children with cerebral palsy. For such personalisation, two 9 years old twin sisters, one with spastic cerebral palsy (C) and a healthy one (H) without any impairments, performed several walks with electromyography (EMG), kinematics and force acquisitions. This paper presents a model of the knee and hip's spastic angular displacement of C during a walk using mechanical differential equations. Two models were designed: one based on the timing of the muscular activation, the other where the timing is defined using a genetic algorithm (GA). These models highlight the spastic contributions of the muscles involved in the walk (agonists and antagonists of the joints studied) and their activations. The amplitude of the activations for both models was carried out using GA.**

Gait cycles were modeled with a determination coefficient (R^2) higher than 84% for both models.

I. Introduction

One of the most common causes of motor disability, especially during childhood, is cerebral palsy (CP) with an incidence of 2.0 to 2.5 per 1000 live births. It is a "group of non-progressive, but often changing, motor impairment syndromes secondary to lesions or anomalies of the brain arising in the early stages of development" [1]. A wide range of prenatal, perinatal, and postnatal isolated or combined factors are considered the main causes of cerebral palsy: hypoxia, gene abnormalities... The severity of the CP can be quantified using Growth Motor Function Classification System (GMFCS) decomposed into 5 levels from the lowest to the highest severity. In this context, the biomechanical analysis of the CP gait aims to better understand the key features of the kinematics and muscle activation. Different CP subtypes exist like ataxic CP, dyskinetic CP and spastic CP which is the subtype studied in this paper. Spasticity is also the most common disabling condition seen in cerebral palsy [2][3] characterized by an abnormal increase in muscle tone creating pathological and involuntary reflexes [4][5] or stiffness of muscle, which can impact the walk of the subject. Spasticity is known to be a "hypersensitive, velocity-dependent response to passive muscle stretch" and also position-dependent as some lower-limb configurations cannot be reached due to the spasticity[6][7][8].

This paper will first focus on the modeling and characterization of the effect of spasticity on a gait cycle of a 9 years old girl called C. who has a spastic CP with a GMFCS level of 2. A gait is a succession of several gait cycles which are determined by two consecutive heel strikes of the same foot [9]. Thus, right and left gait cycles are defined according to the food considered. To model the gait cycle, a double pendulum will be considered composed of the hip and the knee, the joints studied. This model represents the swing phase of the movement which is responsible for the magnitude of the step movement. In this model, we assume that the ankle does not have mobility. This work is then divided into two steps: an experimental one to extract the customized data (muscular activity (EMG) and kinematic data) and a modeling one to recreate the gait using the previous data and a common genetic algorithm (GA) to find the optimal parameters. To simplify the modelization, the right and left gait cycles will be modelized as those cycles can be repeated to reconstruct the walk. In the end, we aim to determine how a spastic gait cycle can be modeled using a double pendulum model. This paper is part of the EXOKID project which aims to design a customized exoskeleton for a child with a specific spastic cerebral palsy and with the final purpose to determine how it can correct or enhance the gait of this child.

II. Related work and contributions

1) Double-pendulum system: Spasticity models are often characterized and designed using data obtained from a pendulum drop test. In [10], a non-linear function representing a couple modeling the contribution of involuntary spastic movements is developed. In [11], spasticity is modeled by a torque representation of muscle hypertonicity and the leg model itself corresponds to a differential equation dependent on the viscoelastic parameters of the agonist and antagonist muscles of the knee. In this continuity, [6] focuses their work on the muscular contribution in the knee angular displacement during a pendulum drop test. The purpose is to clearly indicate that the knee rotation of subjects with spasticity is an active process. They defined additional velocity-feedback torques to emphasize the velocity-dependent aspect of spasticity. An optimization algorithm was used to define the timing and amplitude of those torques without any consideration for muscular activity. This optimization can enhance the performance of the best fitting model but is a source of inaccuracy when it conceals the actual origin of spasticity, which is the involuntary and pathological activation of the muscles [4][5].

All of the cited models studied only the knee joint with a simple pendulum. However, as our final goal is to cor-

[1]Université de Toulouse, CNRS, ICA, ISAE-SUPAERO, Toulouse, France

[2]LAAS-CNRS, Université de Toulouse, CNRS, UPS, France

rect a whole spastic gait, the main contribution of our work is to model a double-pendulum system composed of a thigh/shank/foot system based on the work of [6] and experimental data.

2) Voluntary muscular activations: As we consider a gait cycle and not a simple pendulum drop test, muscular activations torques were added to better represent the normal contribution of the muscles during a movement as in [12]. Two models were then defined: one using the onsets/offsets of the muscular activations as the period of activation for the torques representing voluntary muscular activations and one in which the period of activation is obtained using GA. The amplitude of the spasticity torques was defined using GA.

3) Position-dependent torques: Moreover, additional position-feedback torques are added for the spastic model to bring forward the position-dependent character of spasticity with the same timing as velocity-feedback torques [8].

III. MODELING OF THE SPASTICITY USING A GENETIC ALGORITHM (GA)

A. Method

1) Participants: Two 9 years old twin sisters (C and H) performed a clinical gait analysis (CGA). C has a GMFCS of 2. No maximum voluntary contraction was recorded due to the quick fatigue occurring for C. The anthropometry of C. is presented in Table I. The masses of the segments were computed using regression equations of [13] for children of 9 years old. Before data collection, we obtained informed consent and assent from the parents and the twin, respectively. The parents also have signed an informed agreement that the Declaration of Helsinki is respected during the experiment.

TABLE I

BODY PARAMETERS OF THE TWO TWINS

Parameters	C.
Height (cm)	123
Body weight (kg)	22
Length of the thigh (cm)	33
Mass of the thigh (kg)	2.18
Length of the shank (cm)	28
Mass of the shank (kg)	1.1
Mass of the foot (kg)	0.46

2) Experimental data acquisition: For three-dimensional gait analysis, 48 markers were fixed on subject bone landmarks following the recommendation of the International Society of Biomechanics (ISB) [14][15]. The positions of the reflective markers were recorded by twenty optoelectronic cameras sampled at $200Hz$ (VICON, Oxford's metrics, Oxford, UK). A 6-dimensional external contact wrench applied to the subject by the ground was recorded by five force plates, 2 AMTI platforms and 3 Sensix force platforms, embedded in the ground and sampled at $2000Hz$. (Figure 1 & 2).

Sixteen wireless EMG electrodes were placed on the bodies (Table II) based on the SENIAM recommendations

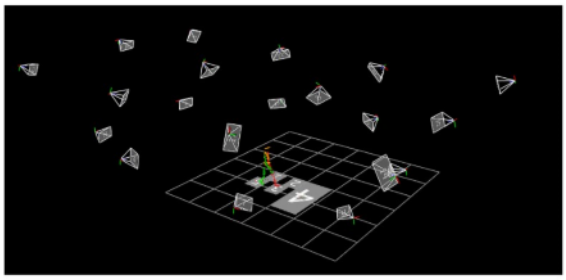

Fig. 1. Experimental setup view from the VICON software. Platform 4 is the Sensix platform and the others are the AMTI force platforms.

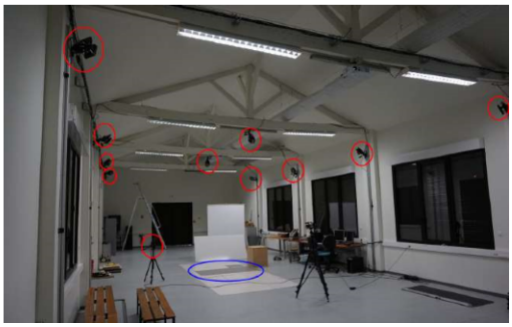

Fig. 2. CREPS laboratory. Cameras are indicated with the red circles and the three platforms with the blue circle

[16] for both legs. Before the electrode application, the skin was shaved and cleaned with alcohol. The electrodes were active parallel bar sensors and were placed in the middle of the muscle, longitudinally to the underlying muscle fibers. Electrodes were secured with adhesive tape before recording. EMG signals were digitized at a $2000Hz$ sampling rate. Table II presents the muscles studied, based on the literature studying muscle activations [17][18][19].

TABLE II

LIST OF THE MUSCLES STUDIED IN THE EXPERIMENT AND THEIR FUNCTION.

Muscles	Acronym	Function
Medial gastrocnemius	M.G	Knee flexor and Ankle extensor
Rectus femoris	R.F	Hip flexor and Knee extensor
Vastus lateralis	V.L	Knee extensor
Semi-tendinous	S.T	Knee flexor and Hip extensor
Biceps femoris	B.F	Knee flexor
Gluteus maximus	G.M	Hip extensor

Linear envelopes for each muscle were obtained by low-pass filtering fully rectified raw EMG signals with a $10Hz$ lowpass filter (2nd order Butterworth, zero lag). The EMG data was then filtered with a 4th-order bandpass Butterworth filter between 20 and $400Hz$. For each participant and each muscle, EMG envelopes were normalized using their mean value over the whole cycle. Muscle activations (onsets and offsets) were determined using an estimation of the proportion p of the signal corresponding to the baseline. The

threshold was set as the mean plus three standard deviations of the $p\%$ lowest values of the sample multiplied by the signal-to-noise ratio. Only periods in which the signal was above the threshold for more than $100ms$ were considered activations. Manual adjustments were done to be more precise on certain signals. Normalization of the EMG signals was done to express each as a percentage of a gait cycle. Markers trajectories were filtered by a 4th-order low pass Butterworth filter with a $10Hz$ cutoff frequency. Gait cycles and events (foot strike and toe-off) were identified manually. The inverse kinematics was performed with OpenSim [20]. Three-dimensional joint angles were computed for each trial (ABC Euler sequence) at the lower limbs.

B. Double pendulum modelization:

Once the data are collected, the thigh and shank trajectories are modeled by using double pendulum equations and the equations defined in [6] (Equations 1 and 2). The foot is considered as a point mass at the end of the shank. The modeling of the knee-muscle spasticity is performed using equations developed in [6]. The spasticity model [6] developed for one degree of freedom (DOF) is used (Equation 5).

For the Hip:

$$\begin{aligned}&\Theta_1''(m_1d_1^2 + I_1 + m_2l_1^2 + m_3l_1^2)+\\&\Theta_2''(m_2l_1d_2cos(\Theta_1 - \Theta_2) - m_3l_1l_2cos(\Theta_1 - \Theta_2))+\\&\Theta_2'^2(m_2l_1d_2sin(\Theta_1 - \Theta_2) + m_3l_1l_2sin(\Theta_1 - \Theta_2))+\\&\qquad g * sin(\Theta_1)(m_1d_1 + m_2l_1 + m_3l_1)\\&\qquad + T_{SpasticityModel} + T_{act} = 0\end{aligned} \quad (1)$$

For the Knee:

$$\begin{aligned}&\Theta_2''(m_2d_2^2 + I_2 + m_3l_2^2)+\\&\Theta_1''(m_2l_1d_2cos(\Theta_1 - \Theta_2) + m_3l_1l_2cos(\Theta_1 - \Theta_2))+\\&\Theta_1'^2(-m_2l_1d_2sin(\Theta_1 - \Theta_2) - m_3l_1l_2sin(\Theta_1 - \Theta_2))+\\&\qquad g * sin(\Theta_2)(m_2d_2 + m_3l_2)\\&\qquad + T_{SpasticityModel} + T_{act} = 0\end{aligned} \quad (2)$$

with:

- $\Theta_{1/2}$, $\Theta'_{1/2}$, $\Theta''_{1/2}$: joint relative angle, velocity and acceleration of the hip joint (1) and the knee joint (2).
- $I_{1/2}$: moment of inertia of the thigh and shank expressed at the center of the joint,
- d_1, d_2: distance between the hip joint(1)/ knee joint(2) and the center of mass of the thigh/shank
- l_1, l_2: length of the thigh and shank
- m_1, m_2, m_3: mass of the thigh, shank and foot respectively
- $T_{SpasticityModel}$: Torques produced by the spasticity model
- T_{act}: Torque vectors produced by voluntary muscular activations

This model does not consider contact forces as external forces to the system. Only gravity is considered here.
T_{act} represents the vectors for each joint of the torques produced by their flexors and extensors. Flexors are considered during flexion and extensors during extension (see Table II for the muscles and their functions). Thus, depending on the joint studied and the phase of the gait (extension or flexion), T_{act} can be defined as follows :
For the hip :

$$T_{actHip} = [S.T_{vector}, G.M_{vector}, V.L_{vector}, R.F_{vector}] \quad (3)$$

For the knee:

$$T_{actKnee} = [S.T_{vector}, M.G_{vector}, B.F_{vector}, R.F_{vector}] \quad (4)$$

They represent the vectors of the corresponding voluntary muscular activations torques (Table II).

In this paper, 2 spastic models are thus defined:

a) Model A: In this model, the timing of the muscular activations torques (T_{act}) corresponds to the real moment of muscular activations obtained from the EMG data. The magnitude of those torques is obtained using GA.

b) Model B: This model corresponds to the optimization of the timing where the muscles are activated : in this case, the torques T_{act} are applied during the entire cycle and their amplitudes are optimized using genetic algorithms.

C. Spasticity model:

The equation of motion of the thigh and the shank are given respectively by equations 1 and 2 for extensors (subscript *e*, when $\Theta' < 0$) and flexors (subscript *f*, when $\Theta' \geq 0$). Thus, extensors are considered during the flexion (spasticity due to the extensor will impact the flexion) and the same reasoning for the flexors.

$$T_{SpasticityModel} = B_{e,f}\Theta' + K_{e,f}\Theta + T_{e,f} + B\Theta' + K\Theta \quad (5)$$

with :

- B_e, B_f: damping coefficients,
- K_e, K_f: stiffness coefficients,
- T_e, T_f: nonlinear stiffness torques defined by [21] as $K1_{e,f}(e^{-K2_{e,f}\Theta} - 1)$
- $B = BE$ or BF: velocity feedback gains for extension (BE) or flexion (BF).
- $K = KE$ or KF: position feedback gains for extension (KE) or flexion (KF).

BE, BF, KE and KF gains are considered applied during the whole gait without interruption and with an unknown magnitude as quantification of the spasticity in a muscular activation cannot be done easily and accurately. Their values are obtained using GA.

The values of the damping coefficients (B_e and B_f) corresponding to the damping part of the muscle fibers, spring coefficients (K_e and K_f), and K1/K2 from the non-linear stiffness torques remain unknown for both hip and knee joints and will be determined using GA.
GA is a method used to solve constrained but also unconstrained optimization problems based on a natural selection process that imitates biological evolution [22]. The goal of GA is to minimize a cost function defined by determining some parameters, chromosomes (Figure 3). A chromosome is a vector of parameters to be determined by the GA.

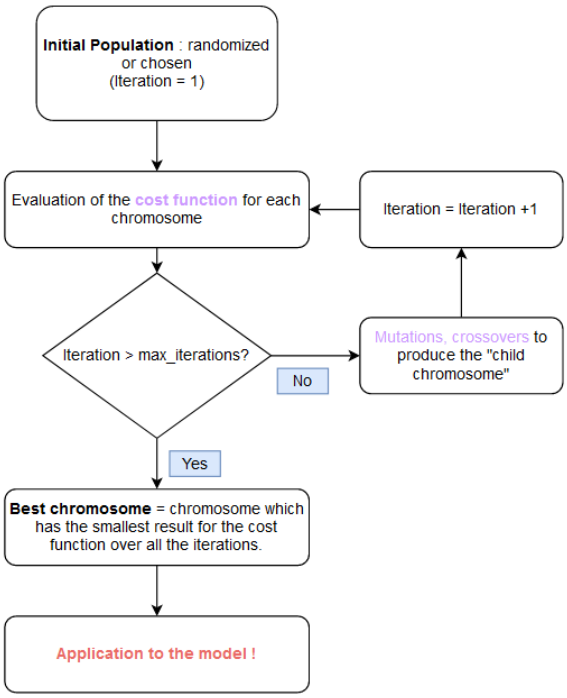

Fig. 3. Flowchart of genetic algorithm (GA).

In this paper, GA aims to identify 2 chromosomes: one for the hip joint (Equation 6) and one for the knee joint (Equation 7) defined as follows:

$$C_{hip} = [K_e, K_f, B_e, B_f, K1_e, K2_e, K1_f, K2_f, BF_{vector}, BE_{vector}, KF_{vector}, KE_{vector}, T_{actHip}] \quad (6)$$

$$C_{knee} = [K_e, K_f, B_e, B_f, K1_e, K2_e, K1_f, K2_f, BF_{vector}, BE_{vector}, KF_{vector}, KE_{vector}, T_{actHip}] \quad (7)$$

with T_{actHip} and $T_{actKnee}$ defined in Equations 3 and 4.

Each cycle has its size representing the number of values per cycle considering the sampling frequency. Thus, BF_{vector}, BE_{vector}, KF_{vector}, KE_{vector}, T_{actHip} and $T_{actKnee}$ have the same size as the gait cycle studied. Indeed, during a gait, muscular activations are expected but it is complicated to determine the part of spasticity in these activations. Therefore, we assumed that spasticity is effective during the whole gait cycle without interruption and with unknown magnitudes.

To determine the parameters of each chromosome, the genetic algorithm was computed with the following parameters:

- Number of parameters to determine : (size of the gait) *10 + 16 parameters for the hip and knee.
- Number of iterations: 5000,
- Number of chromosomes to test at each iteration: 1000,
- Maximum stall generation: 100,
- Tolerance value: $1e^{-5}$

A large number of chromosomes to test at each iteration allows converging quickly to an optimal solution. The number of iterations, the maximum stall generation and tolerance value allow us to consider all possible cases and to stop when there is no significant improvement in the cost function. The parameters presented were chosen after several tests to find a compromise between the accuracy of the results, the convergence of the solution and computing time. The cost function used was based on the difference between modeled angular positions (determined by the resolution of the differential equation using a Newton-Euler method with a time step of $0.05s$) and experimental angular positions of the thigh/shank. The cost function used is based on the coefficient of determination (R^2). The cost function is defined as follows for each joint:

$$Cost\_Function = 1 - R^2 = \frac{\sum_{i=1}^{m} (y_i - \hat{y_i})^2}{\sum_{i=1}^{m} (y_i - \bar{y})^2} \quad (8)$$

with :

- m: number of experimental measurements,
- y_i: value of the experimental measurement i,
- $\hat{y_i}$: corresponding modeled data,
- $\bar{y}$: mean of all the experimental data

At each iteration, the chromosomes are initialized randomly with parameters. The cost function is thus computed and the algorithm continues its calculation until finding an optimal solution. The final cost function used corresponds to the mean of the cost function of the hip and the knee.

In this paper, a single gait of C. was chosen as muscular activations and spasticity vary from one walk to another so the results may be significantly different from one walk to another. This gait is divided into 12 right and left gait cycles. For each model, 2 gait cycles are considered: one right and one left gait cycle. For each gait cycle, the right and left sides of the lower limb are modeled. Those gait cycles were chosen for the lack of issues in their acquisitions. To demonstrate the closeness of those cycles with the other ones, the Normalized Root Mean Square Error (NRMSE) is computed to quantify the difference between the gaits chosen and the others. NRMSE corresponds to the Root Mean Square Error (RMSE) divided by the mean of the

experimental signal (Equation 9). NRMSE goes from 0 to 1 which corresponds to the worst result.

$$RMSE = \frac{\sum_{i=1}^{m} (y_i - \hat{y}_i)^2}{m}; NRMSE = \frac{RMSE}{\bar{y}} \quad (9)$$

Considering all the right gait cycles in this walk, the right gait cycle chosen has an NRMSE of 0.15 with the other right gait cycles. For the left gait cycle, the left gait cycle chosen has an NRMSE of 0.1332. Those results demonstrate that those chosen gait cycles are close enough to the other ones of the walk and can be representative.

D. Data Processing

1) Angular displacement values: Hip and knee angular displacement obtained after the modelization were filtered using a 4th-order lowpass Butterworth filter with a cutoff frequency of $10Hz$.

2) EMG: As a reminder, EMG data were filtered with a-4th order bandpass Butterworth filter between 20 and $400Hz$. Onsets and offsets were determined manually after determining the signal baseline and threshold.

E. Onsets and offsets of the muscular activations

Onsets and offsets of the muscular activations are presented in Table III for a Left Gait Cycle and in Table IV for a Right Gait Cycle. The definition of the onsets and offsets is presented.

TABLE III

VALUES OF THE ONSETS AND OFFSETS OF MUSCULAR ACTIVATIONS DEFINED AS THE PERCENTAGE OF THE LEFT GAIT CYCLE

	1st activation		2nd activation		3rd activation	
Muscles	Onset (%)	Offsets (%)	Onset (%)	Offsets (%)	Onset (%)	Offsets (%)
Rectus femoris	0.06	51	73	99	/	/
Vastus lateralis	0.06	52	80	100	/	/
Semi tendinous	0.05	44	54	60	86	100
Gluteus maximus	0.05	47	56	72	93	100
Medialis gastrocnemius	0.05	5	16	72	88	100
Biceps femoris	0.07	48	59	77	84	99

TABLE IV

VALUES OF THE ONSETS AND OFFSETS OF MUSCULAR ACTIVATIONS DEFINED AS THE PERCENTAGE OF THE RIGHT GAIT CYCLE

	1st activation		2nd activation		3rd activation	
Muscles	Onset (%)	Offsets (%)	Onset (%)	Offsets (%)	Onset (%)	Offsets (%)
Rectus femoris	0.06	45	55	65	76	100
Vastus lateralis	0.06	45	53	66	84	99
Semi tendinous	0.17	45	56	72	85	89
Gluteus maximus	0.96	47	55	75	84	100
Medialis gastrocnemius	2	73	91	99	/	/
Biceps femoris	0.05	49	58	79	88	99

IV. RESULTS

In this part, figures 4 and 5 present the results for the model A and B copared to the experimental data for a right and left gait cycle and for both sides (right and left leg).

A. Model A

As explained, in this model, the timing where the muscular activations torque vectors are applied is based on the onsets and offsets of muscular activations presented in Tables III and IV.

TABLE V

[MODEL A]VALUES OF THE 16 FIRST PARAMETERS COMPOSING THE FINAL CHROMOSOME FOR BOTH LEFT AND RIGHT SIDES OF THE LEFT GAIT CYCLE

Left Side								
Hip	Ke	Kf	Be	Bf	$K1_e$	$K2_e$	$K1_f$	$K2_f$
	-2.5	-1.8	-2.6	2.7	-4.5	-3.8	-4.9	-4.3
Knee	Ke	Kf	Be	Bf	$K1_e$	$K2_e$	$K1_f$	$K2_f$
	-3.6	-1.3	1.0	-1.0	0.9	0.3	1.5	-0.4
Right Side								
Hip	Ke	Kf	Be	Bf	$K1_e$	$K2_e$	$K1_f$	$K2_f$
	4.1	2.8	-3.8	3.0	4.3	3.4	4.9	3.1
Knee	Ke	Kf	Be	Bf	$K1_e$	$K2_e$	$K1_f$	$K2_f$
	-3.3	-3.1	-1.1	-0.8	0.5	1.3	-1.5	-0.9

TABLE VI

[MODEL A]VALUES OF THE 16 FIRST PARAMETERS COMPOSING THE FINAL CHROMOSOME FOR BOTH LEFT AND RIGHT SIDES OF THE RIGHT GAIT CYCLE

Left Side								
Hip	Ke	Kf	Be	Bf	$K1_e$	$K2_e$	$K1_f$	$K2_f$
	-3.1	4.5	-0.5	-0.7	-4.1	-3.2	4.4	4.1
Knee	Ke	Kf	Be	Bf	$K1_e$	$K2_e$	$K1_f$	$K2_f$
	-2.7	-4.4	0.3	-1.9	-1.8	-1.5	-1.9	-0.8
Right Side								
Hip	Ke	Kf	Be	Bf	$K1_e$	$K2_e$	$K1_f$	$K2_f$
	-2.6	-3.2	0.9	-2.2	-3.6	-3.8	4.9	3.2
Knee	Ke	Kf	Be	Bf	$K1_e$	$K2_e$	$K1_f$	$K2_f$
	-4.3	-3.9	1.5	-0.2	-0.7	-0.9	1.6	0.5

1) Left Gait Cycle: Results for the left gait cycle for both sides are presented in Figure 4 and Table V.

a) Right side: The right side has an R^2 equal to 84%: right hip at 80% and right knee at 87%. For BF, BE vectors, the mean value is around -0.55±8.4 and for KF, KE vectors, the mean value is around 0.14±8.4.
For the muscular activation vectors, the mean value is around -0.05±8.7 N.m with a maximum of 13 N.m. For the hip flexors, the mean value is around -0.37 N.m and for the extensors around 0.10 N.m. For the knee flexors, the mean value is around -0.07N.m and for the extensors around -0.37 N.m.

b) Left side: The left side has an R^2 equal to 90%: right hip at 91% and right knee at 89%. For BF and BE vectors, the mean value is around 0.25±8.5 and for KF and KE vectors, the mean value is around 0.21±8.4.
For the muscular activation vectors, the mean value is around 0.06±8.6 N.m with a maximum of 14.6 N.m. For the hip flexors, the mean value is around -0.11 N.m and for the extensors around -0.72 N.m. For the knee flexors, the mean

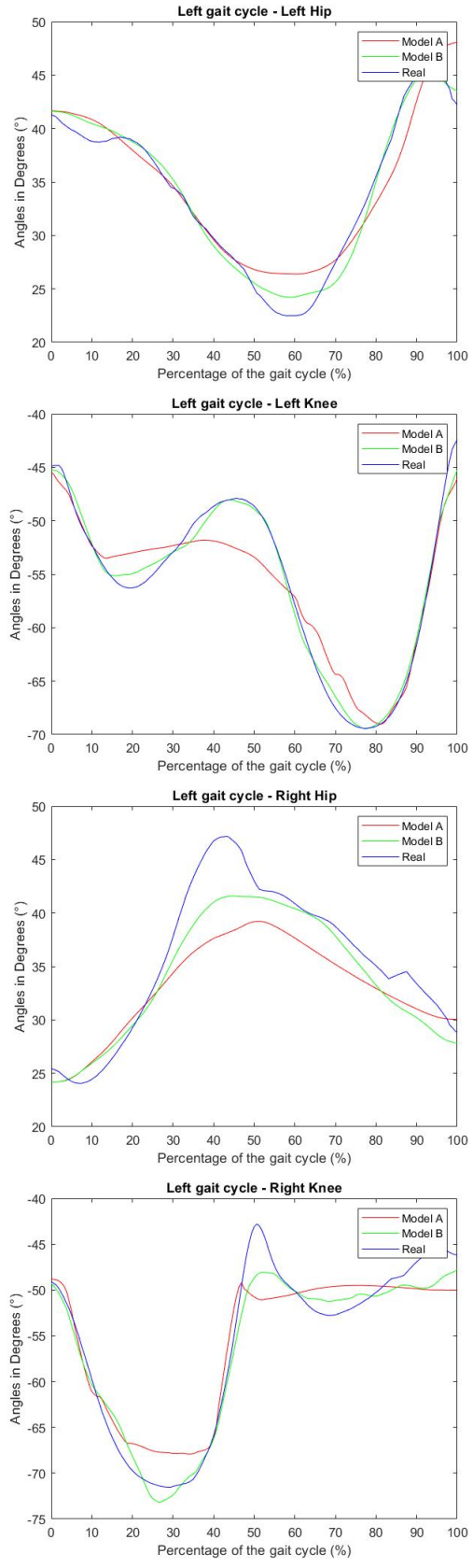

Fig. 4. Simulated and experimental left gait cycle for the left and the right side of the lower limb for both models.

value is around 0.63 N.m and for the extensors around -0.11 N.m.

2) Right Gait Cycle: Results for the right gait cycle for both sides are presented in Figure 5 and Table VI.

a) Right side: The right side has an R^2 equal to 91%: right hip at 94% and right knee at 88%. For BF, BE vectors, the mean value is around -0.06±8.7 and for KF, KE vectors, the mean value is around -0.12±8.6.
For the muscular activation vectors, the mean value is around -0.006±8.6 N.m with a maximum of 12.4 N.m. For the hip flexors, the mean value is around -0.35 N.m and for the extensors around 0.43 N.m. For the knee flexors, the mean value is around -0.04N.m and for the extensors around -0.35 N.m.

b) Left side: The left side has an R^2 equal to 94%: right hip at 91% and right knee at 96%. For BF, BE vectors, the mean value is around 1.29±8.6 and for KF, KE vectors, the mean value is around 0.05±8.7.
For the muscular activation vectors, the mean value is around 0.43±8.67 N.m with a maximum of 14.9 N.m. For the hip flexors, the mean value is around -0.48 N.m and for the extensors around 1.38 N.m. For the knee flexors, the mean value is around 0.33N.m and for the extensors around -0.48 N.m.

Globally for model A, knee parameters and the mean value of BF and BE vectors are close to the values defined in [6]. Results obtained are higher than 80% for the R^2.

B. Model B

TABLE VII
[MODEL B] VALUES OF THE 16 FIRST PARAMETERS COMPOSING THE FINAL CHROMOSOME FOR BOTH LEFT AND RIGHT SIDES OF THE LEFT GAIT CYCLE

Left Side								
Hip	Ke	Kf	Be	Bf	$K1_e$	$K2_e$	$K1_f$	$K2_f$
	-3.8	-4.2	-2.8	0.9	-2.0	-1.3	-3.3	-4.3
Knee	Ke	Kf	Be	Bf	$K1_e$	$K2_e$	$K1_f$	$K2_f$
	-4.3	-2.9	-0.8	-0.9	-0.5	-1.4	-0.2	-0.2
Right Side								
Hip	Ke	Kf	Be	Bf	$K1_e$	$K2_e$	$K1_f$	$K2_f$
	-4.3	0.8	-4.8	-1.6	3.3	1.2	2.5	3.0
Knee	Ke	Kf	Be	Bf	$K1_e$	$K2_e$	$K1_f$	$K2_f$
	3.8	-2.8	-1.5	-1.5	0.9	1.8	-0.4	0.2

Contrary to the previous model, the timing where the muscular activations torque vectors are applied is not based on the onsets and offsets of muscular activations presented in Tables III and IV: they are determined by the GA as the value of the gains for the muscular activations torque vectors.

1) Left Gait Cycle: Results for the left gait cycle for both sides are presented in Figure 4 and Table VII.

a) Right side: The right side has an R^2 equal to 95%: right hip at 93% and right knee at 96%. For BF, BE vectors, the mean value is around -0.04±5.86 and for KF, KE vectors, the mean value is around 0.34±5.6.
For the muscular activation vectors, the mean value is

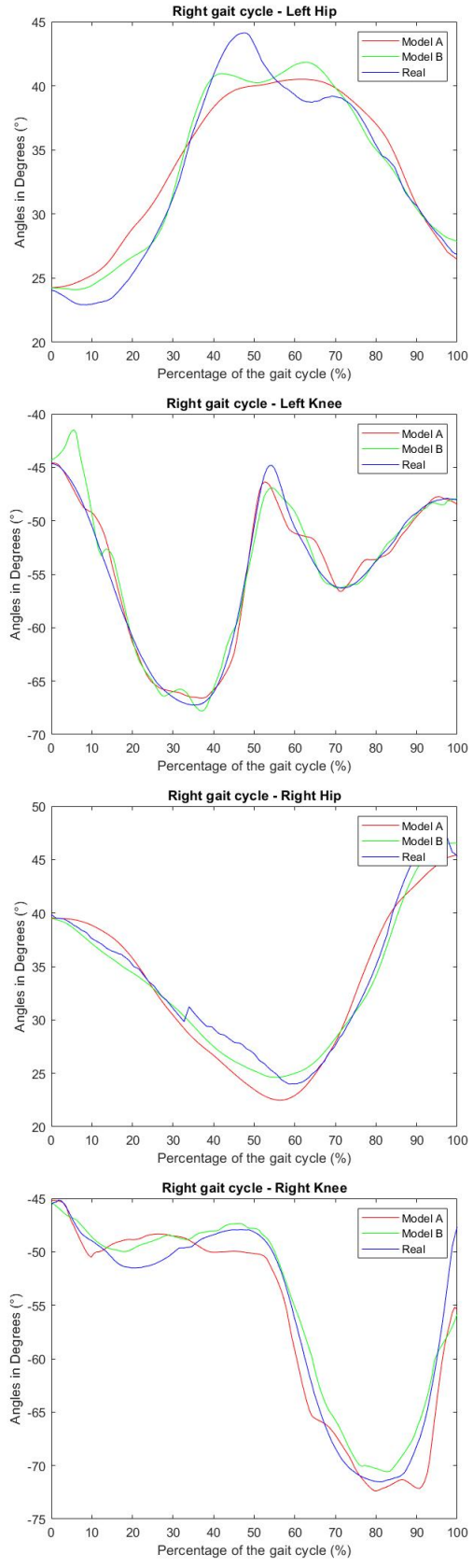

Fig. 5. Simulated and experimental right gait cycle for the left and the right side of the lower limb for both models

TABLE VIII

[MODEL B] VALUES OF THE 16 FIRST PARAMETERS COMPOSING THE FINAL CHROMOSOME FOR BOTH LEFT AND RIGHT SIDES OF THE RIGHT GAIT CYCLE

Left Side								
Hip	Ke	Kf	Be	Bf	$K1_e$	$K2_e$	$K1_f$	$K2_f$
	4.4	-3.0	-3.7	-3.0	-4.3	-2.6	-1.0	2.8
Knee	Ke	Kf	Be	Bf	$K1_e$	$K2_e$	$K1_f$	$K2_f$
	-4.5	-4.7	0.5	-1.0	-1.6	-0.2	0.6	0.9
Right Side								
Hip	Ke	Kf	Be	Bf	$K1_e$	$K2_e$	$K1_f$	$K2_f$
	1.9	0.8	-2.5	-1.3	-1.7	-0.7	-2.8	-3.7
Knee	Ke	Kf	Be	Bf	$K1_e$	$K2_e$	$K1_f$	$K2_f$
	0.6	-4.2	-0.6	-1.9	-1.1	1.1	-1.0	-0.2

around 0.18±5.6 N.m with a maximum of 9.9 N.m. For the hip flexors, the mean value is around 0.64 N.m and for the extensors around 0.37 N.m. For the knee flexors, the mean value is around -0.44N.m and for the extensors around 0.64 N.m.

b) Left side: The left side has an R^2 equal to 98%: right hip at 98% and right knee at 99%. For BF, BE vectors, the mean value is around 0.48±5.7 and for KF, KE vectors, the mean value is around -0.10±5.5.
For the muscular activation vectors, the mean value is around 0.49±5.81 N.m with a maximum of 9.99 N.m. For the hip flexors, the mean value is around 0.67 N.m and for the extensors around 0.77 N.m. For the knee flexors, the mean value is around -0.08N.m and for the extensors around 0.67 N.m.

2) Right Gait Cycle: Results for the right gait cycle for both sides are presented in Figure 5 and Table VIII.

a) Right side: The right side has an R^2 equal to 98% : right hip at 99% and right knee at 97%. For BF, BE vectors, the mean value is around -0.36±8.5 and for KF, KE vectors, the mean value is around -0.27±8.3.
For the muscular activation vectors, the mean value is around 0.21±8.4 N.m with a maximum of 14.1 N.m. For the hip flexors, the mean value is around 0.29 N.m and for the extensors around -0.73 N.m. For the knee flexors, the mean value is around -0.16N.m and for the extensors around 0.29 N.m.

b) Left side: The left side has an R^2 equal to 94%: right hip at 95% and right knee at 92%. For BF, BE vectors, the mean value is around 0.40±8.5 and for KF, KE vectors, the mean value is around 0.59±8.76.
For the muscular activation vectors, the mean value is around 0.01±8.8 N.m with a maximum ok 15 N.m. For the hip flexors, the mean value is around 0.24 N.m and for the extensors around -0.11 N.m. For the knee flexors, the mean value is around -0.04N.m and for the extensors around 0.24 N.m.

In model B, the period of the muscular activations

determined by the GA corresponds to the whole gait: when the muscles should not be active considering values presented in Table III and Table IV, the GA found optimal to create muscular activation torques to better fit the gait cycle. The R^2 results permit demonstrating objectively the relevance of those methods. Model B presents better results than model A: the mean difference is located in the definition of the moment of muscular activations between the two models. The fact that in model B considered a full possible activation during the whole gait can hide 2 issues. First, the manual determination of the offset and onsets of the muscular activations can introduce errors that can modify the timing of real muscular activations which can be compensated by the torques representing the voluntary muscular activations. Thus, a lack of information/parameters used in the model of the gait cycle can be compensated by those new torques as the absence of external forces due to contacts. Nevertheless, the two models present good starting points to model efficiently spastic gait cycles by introducing the contribution of the extensors and flexors muscles.

V. Conclusions

This paper aims to model the left and right gait cycles of a child with spastic cerebral palsy. The modeling of the spasticity using data from EMG, GA and position-dependent/velocity-dependent torques allows us to have similar results compared to the experimental data from C.
This study is a case of study and focused on data of two twin sisters who are not representative of a huge population. This point does not represent a limit to our paper as the aim of the project is to create a customized exoskeleton. The protocol can be enhanced with other twins or other children with spastic cerebral palsy. In this model, there is no mobility for the ankle. In this paper, two gait cycles were studied as cycles can be repeated to create a whole gait. Those simplifications allowed us to focus on the definition of the model. Future works will focus on the control of this gait cycle to make it converge to the one of H. For this purpose, a whole exoskeleton will be modeled and controlled and the interaction of the human and the exoskeleton will be created. Other methods of gait modeling will be tested.

Acknowledgement

The authors would like to thank the Région Occitanie and Université Fédérale Toulouse Midi-Pyrénées (UFTMIP) for their financial support.

Conflict of interest statement

The authors confirm that there are no conflicts of interest regarding the work described in the current manuscript.

References

[1] P. Rosenbaum, "Cerebral palsy: what parents and doctors want to know," *BMJ (Clinical research ed.),*, vol. 326(7396), p. 970–974., 2003.

[2] H. K. Graham, "Pendulum test in cerebral palsy," *Lancet (London, England)*, vol. 355(9222), p. 2184, 2000.

[3] P. O. Pharoah, T. Cooke, I. Rosenbloom, and R. W. Cooke, "Trends in birth prevalence of cerebral palsy." *Archives of disease in childhood*, vol. 62(4), p. 379–384, 1987.

[4] J. W. Lance, "What is spasticity?" *Lancet (London, England)*, vol. 335(8689), pp. 108–115, 1990.

[5] A. Kheder and K. Nair, "Spasticity: pathophysiology, evaluation and management," *Practical neurology*, vol. 12(5), p. 289–298, 2012.

[6] J. Fee, J. W. and R. A. Foulds, "Neuromuscular modeling of spasticity in cerebral palsy," *IEEE transactions on neural systems and rehabilitation engineering : a publication of the IEEE Engineering in Medicine and Biology Society*, vol. 12(1), p. 55–64, 2004.

[7] M. R. Dimitrijevic, "Spasticity," *Scientific Basis of Clinical Neurology*, pp. 108–115, 1985.

[8] Y. N. Wu, H. S. Park, J. J. Chen, Y. Ren, and L. Q. Roth, E. J.and Zhang, "Position as well as velocity dependence of spasticity-four-dimensional characterizations of catch angle," *P. Frontiers in neurology*, vol. 9, 2018.

[9] S. Armand, G. Decoulon, and A. Bonnefoy-Mazure, "Gait analysis in children with cerebral palsy," *EFORT Open Reviews.*, vol. 1, pp. 448–460, 2016.

[10] P. Le Cavorzin, S. Poudens, F. Chagneau, G. Carrault, H. Allain, and P. Rochcongar, "A comprehensive model of spastic hypertonia derived from the pendulum test of the leg," *Muscle Nerve*, vol. 24, pp. 1612–1621, 2001.

[11] T. Bajd and B. Bowman, "Testing and modelling of spasticity," *Journal of biomedical engineering*, vol. 4(2), pp. 90–96, 1982.

[12] H. Wang, P. Huang, X. Li, O. W. Samuel, Y. Xiang, and G. Li, "Spasticity assessment based on the maximum isometrics voluntary contraction of upper limb muscles in post-stroke hemiplegia," *Frontiers in Neurology*, vol. 10, 2019. [Online]. Available: https://www.frontiersin.org/articles/10.3389/fneur.2019.00465

[13] R. K. Jensen, "Body segment mass, radius and radius of gyration proportions of children," *Journal of biomechanics*, vol. 19(5), p. 359–368, 1986.

[14] G. Wu, S. Siegler, P. Allard, C. Kirtley, A. Leardini, and D. Rosenbaum, "Isb recommendation on definitions of joint coordinate system of various joints for the reporting of human joint motion-part i: ankle, hip, and spine." *J.Biomech*, vol. 35(4):543-8, 2002.

[15] G. Wu, "Isb recommendation on definitions of joint coordinate systems of various joints for the reporting of human joint motion–part ii: shoulder, elbow, wrist and hand." *J.Biomech*, vol. 38(5):981, 2005.

[16] H. J. Hermens, B. Freriks, C. Disselhorst-Klug, and G. Rau, "Development of recommendations for semg sensors and sensor placement procedures. journal of electromyography and kinesiology," *International Society of Electrophysiological Kinesiology*, vol. 10(5), p. 361–374, 2000.

[17] D. M. Bojanic, B. Petrovacki-Balj, N. Jorgovanovic, and V. Ilic, "Quantification of dynamic emg patterns during gait in children with cerebral palsy," *Journal of Neuroscience Methods*, vol. 198, p. 325:331, 2011.

[18] K. Steele, M. Munger, B. Shuman, and M. Schwartz, "Repeatability of electromyography recordings and muscle synergies during gait among children with cerebral palsy," *Gait & Posture*, vol. 67, p. 290:295, 2019.

[19] D. Patikas, S. Wolk, W. Schuster, P. Armbrust, T. Dreher, and L. Döderlein, "Electromyographic patterns in children with cerebral palsy: Do they change after surgery?" *Gait & Posture*, vol. 26, p. 362:371, 2007.

[20] S. L. Delp, F. C. Anderson, A. S. Arnold, P. Loan, A. Habib, C. T. John, E. Guendelman, and D. G. Thelen, "Opensim: open-source software to create and analyze dynamic simulations of movement," *IEEE transactions on bio-medical engineering*, vol. 54(11), p. 1940–1950, 2007.

[21] J. M. Winters, "Generalized analysis and design of antagonistic muscle models: Effect of nonlinear muscle properties on the control of fundamental movements," *Ph.D. dissertation, Univ. Calif., Berkeley, CA,*, 1985.

[22] J. H. Holland, *Adaptation in natural and artificial systems: an introductory analysis with applications to biology, control, and artificial intelligence*. MIT press, 1992.